

AD-A102 851

SCIENTIFIC RESEARCH ASSOCIATES INC GLASTONBURY CT  
COMPUTATION OF DISCRETE HOLE FILM COOLING FLOW USING THE NAVIER--ETC(U)  
JUN 81 H GIBELING, J P KRESKOVSKY, W R BRILEY F49620-78-C-0038

F/G 20/13

AFOSR-TR-81-0606

NL

UNCLASSIFIED

100%  
20%  
a/c 851

END  
DATE  
FILED  
9-81  
DTIC

AFOSR-TR- 81 -0606

Report R81-910002-3

AD A102851

COMPUTATION OF DISCRETE HOLE FILM COOLING FLOW  
USING THE NAVIER-STOKES EQUATIONS

H. J. Gibeling, J. P. Kreskovsky, W. R. Briley and H. McDonald  
Scientific Research Associates, Inc.  
P.O. Box 498  
Glastonbury, Connecticut 06033

June 1981

Approved for public release;  
distribution unlimited.

Prepared for:

Air Force Office of Scientific Research

DOCC FILE COPY

*Unclassified*

SECURITY CLASSIFICATION OF THIS PAGE (When Data Entered)

REPORT DOCUMENTATION PAGE		READ INSTRUCTIONS BEFORE COMPLETING FORM
1. REPORT NUMBER <b>AFOSR-TR-81-0606</b>	2. GOVT ACCESSION NO. <b>AD-A102851</b>	3. RECIPIENT'S CATALOG NUMBER
4. TITLE (and Subtitle) Computation of Discrete Hole Film Cooling Flow Using the Navier-Stokes Equations	5. TYPE OF REPORT & PERIOD COVERED Annual Technical Report, 80 April 1 to 81 March 31	
7. AUTHOR(s) H. J. Gibeling, J. P. Kreskovsky, W. R. Briley and H. McDonald	6. PERFORMING ORG. REPORT NUMBER <b>F49620-78-C-0038</b>	
9. PERFORMING ORGANIZATION NAME AND ADDRESS Scientific Research Associates, Inc. P.O. Box 498 Glastonbury, CT 06033	10. PROGRAM ELEMENT, PROJECT, TASK AREA & WORK UNIT NUMBERS <b>61102F 23071/44</b>	
11. CONTROLLING OFFICE NAME AND ADDRESS Air Force Office of Scientific Research Building 410 Bolling AFB, D.C. 20332	12. REPORT DATE June 1981	
14. MONITORING AGENCY NAME & ADDRESS (if different from Controlling Office)	13. NUMBER OF PAGES <b>28</b>	
	15. SECURITY CLASS. (of this report) Unclassified	
	15a. DECLASSIFICATION/DOWNGRADING SCHEDULE	
16. DISTRIBUTION STATEMENT (of this Report)	<p style="text-align: center;"><i>Approved for public release and sale; its distribution is unlimited.</i></p>	
17. DISTRIBUTION STATEMENT (of the abstract entered in Block 20, if different from Report)	Approved for public release; distribution unlimited.	
18. SUPPLEMENTARY NOTES	<p style="text-align: right;"><i>81 814 028</i></p>	
19. KEY WORDS (Continue on reverse side if necessary and identify by block number)	Film Cooling Navier-Stokes Equations Zone Embedding Interactive Boundary Conditions	
20. ABSTRACT (Continue on reverse side if necessary and identify by block number)	<p>An analysis and computational procedure are described here for predicting flow and heat transfer which results from coolant injection through a single row of round holes oriented at an angle to a flat surface with the injection and free stream velocity vectors coplanar. The present method solves the compressible Navier-Stokes equations and utilizes "zone embedding", surface-oriented coordinates, interactive boundary conditions, and an efficient split LBI scheme. The approach treats the near-hole flow region where the film</p>	

unclassified

SECURITY CLASSIFICATION OF THIS PAGE(When Data Entered)

cooling flow is initially established. A sample laminar flow calculation is presented for an injection angle of 45 degrees and a ratio of normal injection to free stream velocity of 0.1. Selected results are compared with previous calculations for the normal injection case. Although the present results do not include heat transfer predictions, details of the interaction between injectant and main stream flow near the hole exit are in qualitative agreement with experimental observations for other flow conditions.

unclassified

SECURITY CLASSIFICATION OF THIS PAGE(When Data Entered)

## TABLE OF CONTENTS

	Page
ABSTRACT. . . . .	1
INTRODUCTION. . . . .	2
PREVIOUS WORK . . . . .	3
THE PRESENT APPROACH. . . . .	5
METHOD OF SOLUTION. . . . .	6
Differencing Procedures. . . . .	8
Split LBI Algorithm. . . . .	8
Computed Results . . . . .	10
Summary and Concluding Remarks . . . . .	12
REFERENCES. . . . .	13
FIGURES . . . . .	14

Accession No.	1
NTIS GRAIL	1
DFIC TAB	1
Unannounced	1
Justification	1
By _____	1
Distribution	1
Approved by _____	1
Date _____	1

*[Handwritten signature]*

AIR FORCE OFFICE OF SCIENTIFIC RESEARCH (AFSC)  
 NOTICE OF TRANSMITTAL TO DDC  
 This technical report has been reviewed and is  
 approved for public release IAW AFR 190-12 (7b).  
 Distribution is unlimited.  
 A. D. BLOUSE  
 Technical Information Officer

Computation of Discrete Hole Film  
Cooling Flow Using the Navier-Stokes Equations  
by

ABSTRACT

An analysis and computational procedure are described here for predicting flow and heat transfer which results from coolant injection through a single row of round holes oriented at an angle to a flat surface with the injection and free stream velocity vectors coplanar. The present method solves the compressible Navier-Stokes equations and utilizes "zone embedding", surface-oriented coordinates, interactive boundary conditions, and an efficient split LBI scheme. The approach treats the near-hole flow region where the film cooling flow is initially established. A sample laminar flow calculation is presented for an injection angle of 45 degrees and a ratio of normal injection to free stream velocity of 0.1. Selected results are compared with previous calculations for the normal injection case. Although the present results do not include heat transfer predictions, details of the interaction between injectant and main stream flow near the hole exit are in qualitative agreement with experimental observations for other flow conditions.

## INTRODUCTION

To achieve higher turbine efficiencies, designers have been forced to deal with high turbine inlet temperatures which may exceed structural limitations of available materials used for blading unless some method of cooling these blades is introduced. Various cooling schemes have been devised to ensure that the structural integrity of the blades remain intact when exposed to a high temperature environment for prolonged periods of time. One of the more promising schemes is discrete hole film cooling, wherein cooling air is injected through either a single row or multiple staggered rows of holes, to provide a protective layer of cool air between the blade surface and hot mainstream gases. Discrete hole film cooling is better suited to the high temperatures of advanced high performance engines than the current convectively cooled blades found in commercial engines. A large number of parameters can be varied to obtain a configuration which optimizes heat transfer and aerodynamic characteristics, including hole shapes and patterns, injection angles and rates, surface curvature, coolant temperatures, and mainstream boundary layer characteristics. Since experimental determination of optimal configurations is costly, a computational procedure which could be used to screen alternative configurations without experimental testing would be of considerable value. An analysis and computational procedure is described here for predicting flow and heat transfer which results from coolant injection through a single row of round holes oriented at a non-normal angle to a flat surface. The work discussed herein is an extension of a previous effort which considered only normal injection through a single row of round holes. This study provides an improved understanding of the film cooling process, particularly in the near-hole region, and represents the second step toward development of a computer program capable of predicting heat transfer and aerodynamic loss levels associated with discrete hole film cooling on gas turbine blades.

## PREVIOUS WORK

Previous experimental work on film cooling flow has consisted mainly of flow visualization studies and measurements of film cooling effectiveness downstream of the coolant injection hole for a variety of flow conditions. For example, Colladay and Russell [1] performed a flow visualization study of discrete hole film cooling in three different hole configurations, to obtain a better understanding of flow behavior associated with coolant injection. They considered injection from discrete holes in a three-row staggered array with five-diameter spacing and three-hole angles: (1) normal to the surface, (2) slanted 30 degrees to the surface but aligned (coplanar) with the free stream, and (3) slanted 30 degrees to the surface and 45 degrees laterally to the free stream. For flow conditions typical of gas turbine applications, Colladay and Russell observed that normal injection is subject to flow separation even at low injection rates, that slanted injection works well except at high injection rates, and that compound slanted-yawed injection is less susceptible to separation but tends to promote entrainment of free stream fluid (which augments heat transfer) and to increase secondary flow losses. These experimental observations emphasize the importance of interaction between the injected fluid and the free stream.

Kadotani and Goldstein [2] have performed experimental measurements for discrete hole film cooling through a row of holes having three-diameter lateral spacing, inclined at 35 degrees to the injection surface, and coplanar with the free stream. They considered a variety of flow conditions and varied boundary layer thickness and injection rates, as well as Reynolds number and turbulence properties. They measured lateral and streamwise distributions of film cooling effectiveness downstream of injection, and also measured mean velocity and temperature in a transverse plane normal to the free stream and located at the downstream edge of the injection holes. Kadotani and Goldstein deduced from their measurements that reversed flow is present near the injection hole even for injection rates as low as 0.35, and that the size and strength of the reversed flow increases with increasing boundary layer thickness. They also found that the approaching boundary layer thickness significantly affects the flow behavior and lateral variation of film cooling effectiveness, particularly near the injection hole.

In a prior study of injection through a single array of round holes oriented normal to a flat surface, Kreskowsky, Briley and McDonald [3] solved the compressible Navier-Stokes equations utilizing surface oriented coordinates and an efficient, consistently split LBM scheme. This study, which represented the first phase of the current effort, adopted flexible interactive boundary conditions in a zone embedding approach to solve the near hole flow region including the flow within the coolant hole. A sample laminar calculation yielded predictions of the interaction between the injectant and main stream flow which were in qualitative agreement with experimental observations.

The only other previous computational study known to the authors which treated the discrete hole film cooling problem using a three-dimensional calculation procedure is that of Bergoles, Gosman and Launder [4], who applied the approximate "partially parabolic" calculation procedure of Pratap & Spalding [5] for the case of laminar flow. This calculation procedure neglects streamwise diffusion and employs iterated forward marching solution of three approximate momentum equations. The procedure begins with a "guessed" pressure field and performs iterated forward marching sweeps of the three-dimensional flow field, solving the approximate momentum equations and utilizing various strategies to modify or correct the pressure field, so as to improve the continuity balance. Since the calculation procedure is based on forward marching, the flow region within the coolant injection hole is excluded from the computational domain, and instead, the coolant velocity distribution is specified at the hole exit as a two-dimensional uniform stream at a prescribed injection angle. Bergoles, Gosman and Launder made flow calculations for several flow conditions, including different injection angles.

## THE PRESENT APPROACH

The present study focuses on the near-hole flow region where the film cooling flow is initially established and where local hot spots may occur. Since the flow field surrounding injection may involve separation and reversed flow relative to the free stream, and since directional and/or other properties of the flow which might permit simplifying assumptions are not clearly evident, the present approach is based on numerical solution of the three-dimensional compressible Navier-Stokes equations. The governing equations in Cartesian coordinates are cast into strong conservation form using a Jacobian transformation to obtain the governing equations in a general nonorthogonal coordinate system. The coordinate system used in the present study is a skewed elliptical-polar coordinate system which is not aligned with the free stream flow. However, all solid surfaces and computational boundaries lie along coordinate lines in the transformed coordinate system.

In selecting the computational domain, a "zone embedding" approach is adopted whereby attention is focused on a subregion of the overall flow field in the immediate vicinity of the discrete hole coolant injection. At the curved boundaries located within the free stream region, interactive boundary conditions which permit inflow and outflow of shear layers and the compressible inviscid free stream are derived from an assumed flow structure. Since details of the coolant velocity distribution at the hole exit are not known a priori and presumably will depend on an interaction between the coolant and the free stream flow, the computational domain is chosen to include the flow region within the coolant hole as well as that exterior to the hole. Including the flow region within the coolant hole permits the interaction between the coolant and free stream flows and its important influence near the hole to be determined as part of the final solution, without the need for simplifying assumptions. The governing equations are solved by an efficient and noniterative time-dependent "linearized block implicit" (LBI) scheme.

## METHOD OF SOLUTION

### Zone Embedding and Interactive Boundary Conditions

The skewed elliptical polar coordinate system  $(r, \theta, z')$  and the computational grid used in the present calculations are shown in Fig. 1, where  $z'$  is the sheared coordinate variable. The polar coordinates  $(r, \theta)$  in the surface plane ( $z/R=0$ ) vary from circular at the origin to elliptical at the edge of the coolant hole to circular again at the outer boundary of the domain ( $r/R=5$ ). The latter choice is not a necessity, and the outer transverse boundary location (at  $\theta = \pi/2$ ) may be selected to determine the coolant hole spacing. The injection angle chosen for the present case is 45 degrees. Above the hole the coordinate system skewing angle was gradually changed from 45 to 90 degrees at the outer boundary ( $z/R=5$ ) allowing symmetry conditions to be easily applied, so that the flow represented is that of opposing coolant holes located on parallel flat plates with spacing  $h/R=10$ . Velocity boundary conditions at no-slip and symmetry surfaces are straightforward and self-explanatory. The remaining condition at the no-slip surface in the plane of the hole ( $z/R=0$ ) was taken as the normal (z-cartesian) momentum equation, and within the coolant hole  $\partial p/\partial n = 0$  was applied, where  $n$  is the normal direction at any surface. The latter condition at a no-slip surface is correct to order  $Re^{-1}$  for viscous flow at high Reynolds number.

The treatment of inflow and outflow conditions is an obstacle to be overcome within the zone embedding approach. This problem was successfully treated for the normal injection case by Kreskovsky, Briley and McDonald [3] and thus their general approach is followed in the present study. At the computational boundaries located within the free stream region, interactive inflow-outflow boundary conditions are derived from an assumed flow structure and physical approximations following Ref. 3. The assumed inflow structure consists of a uniform potential flow core velocity  $\bar{U}_1$ , two-dimensional estimates of the boundary layer displacement thickness  $\delta^*(x)$  on the flat surface, and finally an estimate of the blockage correction factor  $B(x)$ . The boundary layer displacement thickness  $\delta^*(x)$  is estimated from the known development of flow between parallel flat plates (e.g. Kreskovsky and Shamroth [6] and references). Given this estimate of  $\delta^*(x)$ , the boundary layer thickness is approximated by the Blasius relationship  $\delta(x) = 5/1.72 \delta^*(x)$  and the blockage factor is given by  $B(x) = [H/2R - \delta^*(x)]^{-1}$ . Finally, boundary layer velocity profile shapes  $f(z/\delta)$ ,  $0 \leq f \leq 1$  are defined from

von-Karman Pohlhausen polynomial profiles and the boundary layer thickness  $\delta(x)$ . The initial velocity vector  $\bar{U}$  at  $t=0$  is defined by

$$\bar{U}(r, \theta, z) = \bar{U}_I B(x) f\left[\frac{z}{\delta(x)}\right] \quad (1)$$

At the inflow boundary, a "two-layer" boundary condition is devised such that stagnation pressure  $P_o$  is fixed at the free stream reference value  $(P_o)_r$  in the core flow region ( $z > \delta$ ), and the cartesian velocity  $u$  is set by  $u = u_e(x, t) f(z/\delta)$  for  $z \leq \delta$ . The local free stream velocity  $u_e$  is chosen consistent with the free stream total pressure  $P_o$ , total temperature  $T_o$ , and the local static pressure  $p_e$  at a specified point on the boundary, such that the initial distribution of  $u_e$  is maintained:

$$u_e(x, t) = u_e(x, t=0) \cdot f(P_o, T_o, p_e) \quad (2)$$

and the function  $f$  follows from isentropic relations. The static pressure at the point in question is determined as part of the solution and is updated after each time step. The latter application of the two-layer boundary condition is a variation of the condition used by Ref. 3, which was required because of the skewed nature of the computational domain. The remaining inflow conditions are  $v = 0$ ,  $\partial^2 w / \partial n^2 = 0$ , and  $\partial^2 c_p / \partial n^2 = g(\theta, z)$  where  $g$  is the value of this quantity at  $t = 0$  with  $c_p$  defined as  $(1 - B \bar{U}_I \cdot \bar{U}_I)$ , which is its value from the potential flow corrected for estimated blockage.

For outflow conditions, second derivatives of each computed velocity component are set to zero and the static pressure is imposed and updated after each time step from an assumed form which varies linearly with  $x$  from a fixed value at the downstream limit of the flow region ( $r/R=5$ ,  $\theta=0$ ) to a value at  $\theta=\pi/2$  which is consistent with the upstream total pressure and the local free-stream dynamic head. At the inflow boundary within the coolant hole, the normal velocity component is given a specified velocity profile distribution with uniform core region, and remaining velocity components are extrapolated using zero second derivative. The remaining condition is  $\partial^2 p / \partial n^2 = 0$ .

The foregoing interactive inflow-outflow boundary conditions are designed to permit the mass flux through the computational domain to adjust to both the imposed downstream static pressure and to viscous losses present in the flow, while maintaining a specified flow structure based on physical assumptions consistent with the flow problem under consideration. Various refinements in the interactive boundary conditions are possible, such as including the effect of local pressure gradient on boundary layer growth and profile shape.

### Differencing Procedures

The differencing procedures used are a straightforward adaptation of those used by Briley and McDonald [7] in cartesian coordinates for flow in a straight duct. Although the present procedure can ultimately be used to compute local heat transfer distributions, the present study has focused on methodology for treating the fluid flow near and within an injection hole. Accordingly, for the present, the fluid stagnation enthalpy is assumed constant for reasons of economy. The definition of stagnation enthalpy and the equation of state for a perfect gas can then be used to eliminate pressure and temperature as dependent variables, and solution of the energy equation is unnecessary. The continuity and three cartesian momentum equations are solved in the  $(r, \theta, z')$  coordinate system with density and the cartesian velocity components  $(u, v, w)$  as dependent variables. Three-point central differences were used for spatial derivatives, and second-order artificial dissipation terms are added as in [7] to prevent spatial oscillations at high cell Reynolds number. This treatment lowers the formal accuracy to first order but does not seriously degrade accuracy in representing viscous terms in thin shear layers. Analytical coordinate transformations were used to provide increased resolution of critical portions of the flow field. These coordinate transformations serve to concentrate grid points near the flat surface, near the hole surface, near the hole exit, and in the region just downstream of the hole. Derivatives of geometric data were determined numerically for use in the strong conservation form of the difference equations.

### Split LBI Algorithm

The numerical algorithm used is the consistently-split "linearized block implicit" (LBI) scheme developed by Briley and McDonald [7,8] for systematic use in solving systems of nonlinear parabolic-hyperbolic partial differential equations (PDE's). To illustrate the algorithm, let

$$(\phi^{n+1} - \phi^n)/\Delta t = \beta D(\phi^{n+1}) + (1-\beta) D(\phi^n) \quad (3)$$

approximate a system of time-dependent nonlinear PDE's (centered about  $t^{n+\frac{1}{2}\Delta t}$ ) for the vector  $\phi$  of dependent variables, where  $D$  is a multidimensional vector spatial differential operator, and  $t$  is a discretized time variable such that  $\Delta t = t^{n+1} - t^n$ . A local time linearization (Taylor expansion about  $\phi^n$ ) is introduced, and this serves to define a linear differential operator  $L$  such that

$$D(\phi^{n+1}) = D(\phi^n) + L^n(\phi^{n+1} - \phi^n) + O(\Delta t^2) \quad (4)$$

Eq. (3) can thus be written as the linear system

$$(I - \beta \Delta t L^n)(\phi^{n+1} - \phi^n) = \Delta t D(\phi^n) \quad (5)$$

The multidimensional operator  $L$  is divided into three "one-dimensional" sub-operators  $L = L_1 + L_2 + L_3$  (associated here with the three coordinate directions), and Eq. (5) is split as in the scalar development of Douglas and Gunn [9] and is written as

$$(I - \beta \Delta t L_1^n)(\phi^* - \phi^n) = \Delta t D(\phi^n) \quad (6a)$$

$$(I - \beta \Delta t L_2^n)(\phi^{**} - \phi^n) = \phi^* - \phi^n \quad (6b)$$

$$(I - \beta \Delta t L_3^n)(\phi^{***} - \phi^n) = \phi^{**} - \phi^n \quad (6c)$$

$$\phi^{n+1} = \phi^{***} + O(\Delta t^3) \quad (6d)$$

If spatial derivatives appearing in  $L$  are replaced by three-point difference formulas, then each step in Eqs. (6a-c) can be solved by a block-tridiagonal "inversion". Eliminating the intermediate steps in Eqs. (6a-d) results in

$$(I - \beta \Delta t L_1^n)(I - \beta \Delta t L_2^n)(I - \beta \Delta t L_3^n)(\phi^{n+1} - \phi^n) = \Delta t D(\phi^n) \quad (7)$$

which approximates Eq. (5) to order  $\Delta t^3$ . Complete derivations are given in [7,8]. It is noted that Beam & Warming [10] have reformulated this algorithm as a widely-used "delta form" approximate factorization scheme whose two-level form is identical to Eq. (6).

Finally, it is noted that a special treatment for radial boundary conditions is needed at the polar axis  $r=0$  of the coordinate system being used. As a result of the splitting of Eq. (5), a separate (i.e., "multivalued") radial boundary condition is needed for each  $r$ -implicit step of the split algorithm. As discussed in Ref. 3 symmetry conditions are valid at  $r=0$  and provide a usable radial boundary condition for the implicit step which corresponds to  $\theta=\pi/2$ . Consequently, for each  $z$  value, the  $r$ -implicit steps are reordered so as to solve the  $\theta=\pi/2$  step first, using symmetry conditions. This defines implicit

values for the dependent variables at  $r=0$  which in turn are used to specify function boundary conditions for the remaining  $r$ -implicit steps ( $\theta \neq \pi/2$ ), whose order is immaterial.

#### Computed Results

To illustrate the application of the present approach to the discrete hole film cooling problem, a sample calculation has been computed for laminar flow with coolant injected at 45 degrees to the free stream. Although the present results are limited to laminar flow with the coolant injection velocity coplanar with the free stream, this approach may be extended to treat turbulent flow, heat transfer, and a coolant injection velocity not coplanar with the free stream. In the flow considered, the ratio of average coolant velocity to average main stream velocity is 0.1, the free stream Reynolds number based on duct width is 400, and the reference Mach number is 0.3. The Reynolds number based on hole diameter is 80. The thickness  $\delta/R$  of the approaching boundary layer is 1.8. The solution converged in about 50 time steps and with a  $14 \times 19 \times 15$  grid required about 24 minutes of CDC 7600 CP time.

Selected results from this sample calculation are shown in Figs. 2-7. For comparison purposes certain results from the normal injection case presented in Ref. 3 are reproduced in Figs. 8-11. A vector plot of velocity in the vertical symmetry plane ( $\theta=0, \pi$ ) passing through the center of the coolant hole is shown in Fig. 2. It can be seen that most of the coolant flow leaves the hole near its downstream edge, and for this particular set of flow conditions, the coolant flow does not penetrate beyond the mainstream boundary layer. Comparing the velocity vectors with those from the normal injection case, Fig. 8, it can be seen that the penetration of the jet into the main flow is less in the  $45^\circ$  injection case, as expected. Contours of velocity components comprising the velocity vectors in Fig. 2 are shown in Fig. 3. It can be seen that the streamwise component is not greatly disturbed by the coolant injection at this ratio of injectant to free stream velocity (0.1). However, it is clear from the contours of vertical velocity that there is significant local interaction between the main stream and coolant stream near the hole exit, and that this interaction affects the coolant flow within the hole. It can be seen from these contours that the coolant velocity profile becomes highly distorted at the hole exit plane ( $z/R=0$ ). The streamwise and vertical velocity contours from the normal injection case are shown in Fig. 9, from which it is evident the primary difference in the two cases occurs in the vicinity of the upstream edge

of the coolant hole. There in the  $45^\circ$  injection case the vertical component of velocity varies rapidly near the upstream side of the hole in a manner similar to that occurring along the downstream side as the hole exit plane is approached. This behavior was not present in the normal injection case, Fig. 9b, and presumably the phenomenon predicted in the  $45^\circ$  injection case is due to the occurrence of a low pressure region near the upstream edge of the coolant hole at the exit plane. Further verification of this behavior would require recalculation with a refined computational mesh. The present approach provides a means for detailed prediction of this local interaction, by including a portion of the hole within the computed flow region. It is also noted that the present results did not predict a reversed flow region downstream of the hole, probably due to the relatively low injection rate and the injection angle.

A further indication of the coolant injection flow is given in Fig. 4, where contours of the vertical velocity (normal to the flat surface) are shown for selected horizontal planes. Note that the location of the coolant hole at  $z/R=0$  is shifted to the left in the figures, since the grid is skewed in the  $z$ -direction. A vector plot of velocity in a horizontal plane one grid point above the hole exit ( $z/R=0.15$ ) is shown in Fig. 5, and this figure shows the extent of lateral flow deflection present in the computed results. The corresponding vector plot from the normal injection case is shown in Fig. 10, where comparison reveals the expected reduced lateral deflection of the main stream flow in the  $45^\circ$  injection case. Contours of the streamwise ( $u$ ) and transverse ( $v$ ) components of velocity shown in Fig. 6 at  $z/R=0.15$  further illustrate the influence of the coolant injection on the mean flow boundary layer. Finally, vector plots of secondary velocity in vertical planes perpendicular to the main flow direction are shown in Fig. 7 for several streamwise locations upstream, within, and downstream of the hole. These plots provide an indication of the secondary flow and fluid entrainment induced by the coolant injection. Again, this behavior is qualitatively similar to the secondary flow patterns observed in the normal injection case, Fig. 11.

A problem which makes a detailed assessment of the predictions difficult is the occurrence of pressure oscillations in the computations near the edge of the coolant hole exit plane. Although the solution remains stable in their presence the oscillations do make a quantitative assessment of the results in the vicinity of the coolant hole difficult. The oscillations appear to emanate from the edge of the hole which is a reentrant corner in the computational

$(r, z')$  plane for each value of  $\theta$ . These corner points are presently treated in the split LBI framework using the "double-value" concept, whereby values for each variable at the corner are associated with the direction from which the corner is approached. In the present case the velocities are identically zero at the corner, so only density and pressure are multivalued. This approach tends to reduce the region of solution contamination around the corner, however, an alternate approach to the double values may be necessary to reduce the oscillations and obtain quantitatively accurate results.

#### Summary and Concluding Remarks

A computational procedure has been described for predicting flow and heat transfer which results from coolant injection through round holes oriented at 45 degrees to a flat surface. The procedure solves the compressible Navier-Stokes equations without simplifying assumptions, and includes portions of the flow field both within the coolant hole and exterior to the hole. Zone embedding and interactive boundary conditions are used to achieve economy by limiting the solution domain to the near-hole flow region, where simplifying assumptions are undesirable because of local interaction and reversed flow. A sample coarse-mesh calculation has been obtained for laminar adiabatic flow with a ratio of normal injection to free stream velocity of 0.1. This calculation demonstrates the general capability of the present procedure for treating coolant injectant flows without making simplifying assumptions in the near-hole flow region. The results obtained for the 45 degree injection case are qualitatively reasonable, and the differences observed between this case and the normal injection case appear to be physically plausible. A more detailed evaluation of the procedure and its capabilities would require fine-mesh calculations and consideration of nonadiabatic flows and other coolant velocity ratios. The present procedure can also be extended to treat compound injection through holes not coplanar with the free stream, by modifying the treatment of the coordinate system singular points ( $r=0$ ) and by solving the equations over the full angular range ( $0 \leq \theta \leq 2\pi$ ) with periodic boundary conditions.

#### REFERENCES

1. Colladay, R.S. and Russell, L.M.: Streakline Flow Visualization of Discrete-Hole Film Cooling With Normal, Slant, and Compound Angle Injection, NASA TN D-8248, September, 1976.
2. Kadotani, K. and Goldstein, R.J.: Effect of Mainstream Variables on Jets Issuing from a Row of Inclined Round Holes, Journal of Engineering for Power, Vol. 101, 1979, p. 299.
3. Kreskovsky, J.P., Briley, W.R. and McDonald, H.: Computation of Discrete Hole Film Cooling Flow Using the Navier-Stokes Equations. Annual Technical Report, Contract F49620-78-C-0038, SRA Report R80-910002-2, May 1980.
4. Bergeles, G., Gosman, A.D. and Launder, B.E.: The Prediction of Three-Dimensional Discrete-Hole Cooling Processes: 1-Laminar Flow, ASME Paper 75-WA/Ht-109, 1975.
5. Pratap, V.S. and Spalding, D.B.: Fluid Flow and Heat Transfer in Three-Dimensional Duct Flows, Int. J. Heat and Mass Transfer, Vol. 19, 1976, p. 1183.
6. Kreskovsky, J.P. and Shamroth, S.J.: An Implicit Marching Method for the Two-Dimensional Reduced Navier-Stokes Equations at Arbitrary Mach Number. Computer Methods in Applied Mechanics and Engineering, Vol. 13, 1978, p. 307.
7. Briley, W.R. and McDonald, H.: Solution of the Multidimensional Compressible Navier-Stokes Equations by a Generalized Implicit Method. Journal of Computational Physics, Vol. 24, 1977, p. 372.
8. Briley, W.R. and McDonald, H.: On the Structure and Use of Linearized Block Implicit Schemes. J. Computational Physics, Vol. 34, No. 1, 1980, p. 54.
9. Douglas, J. and Gunn, J.E.: A General Formulation of Alternating Direction Methods. Numerische Mathematik, Vol. 6, 1964, p. 428.
10. Beam, R.M. and Warming, R.F.: An Implicit Factored Scheme for the Compressible Navier-Stokes Equations. AIAA Journal, Vol. 16, 1978, p. 393.

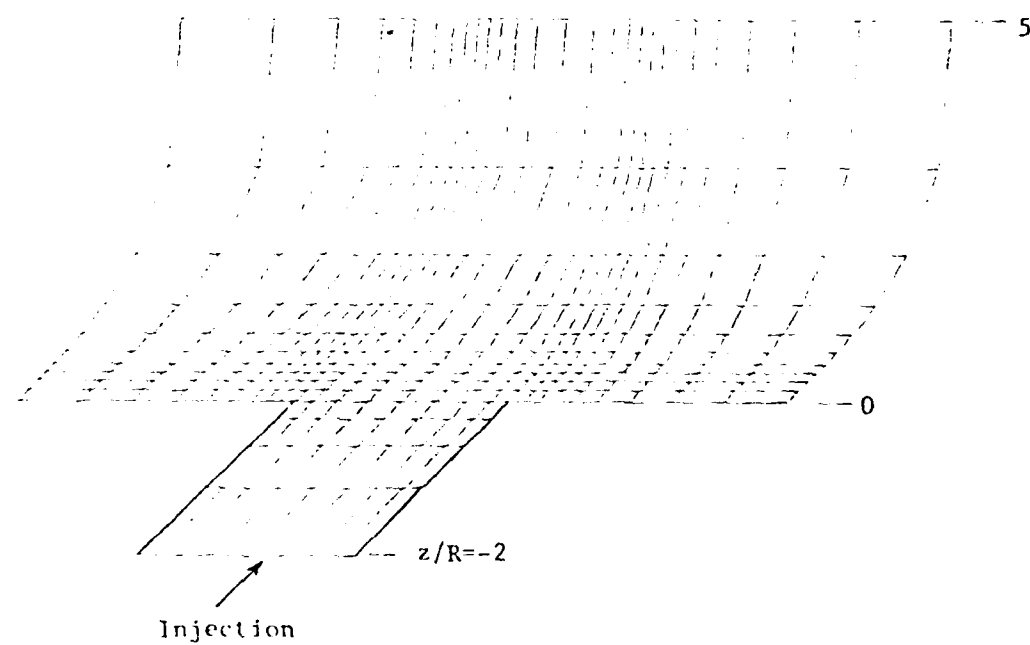
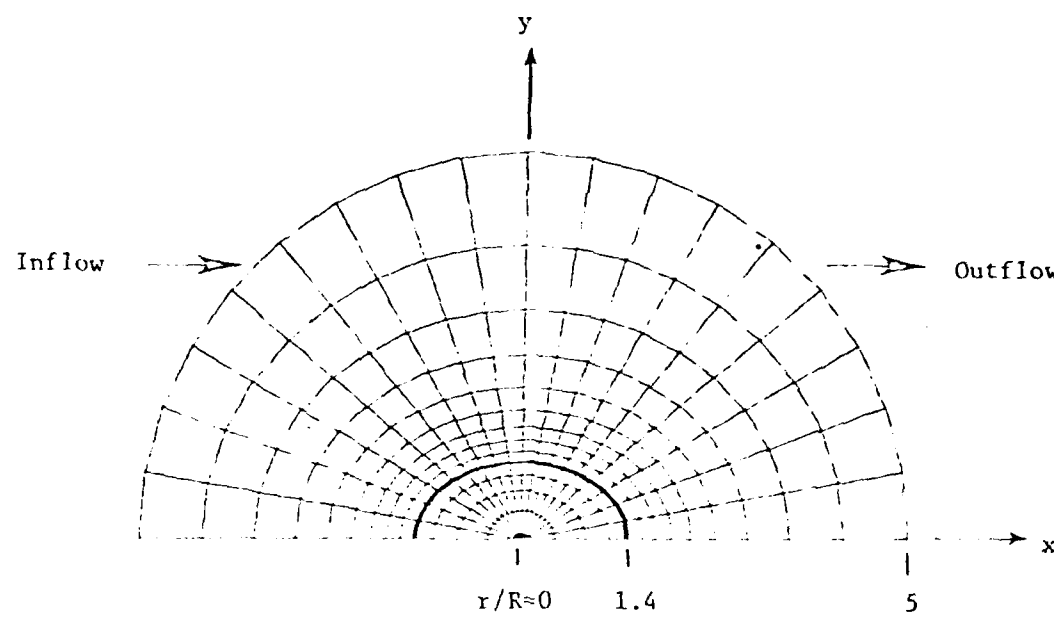


Fig. 1 - Geometry, Coordinate System and Computational Grid,  
45° Injection.

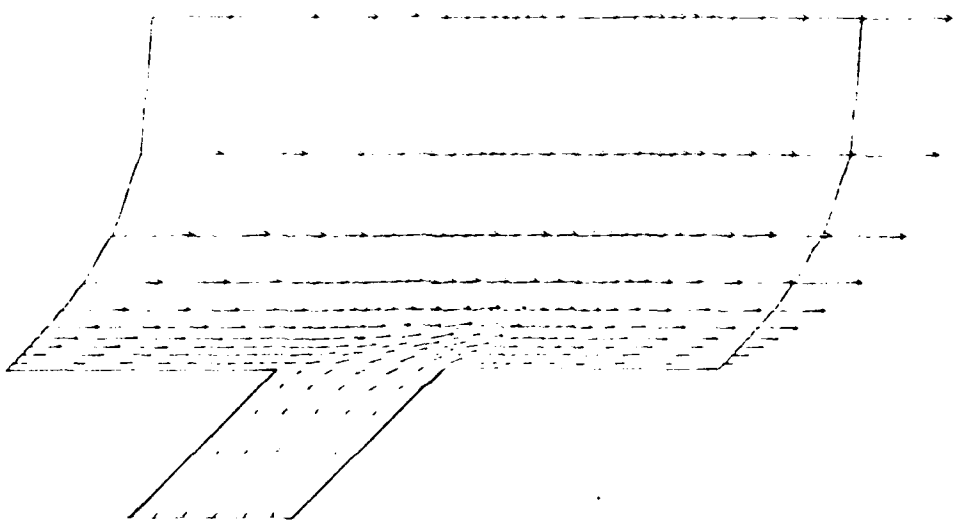
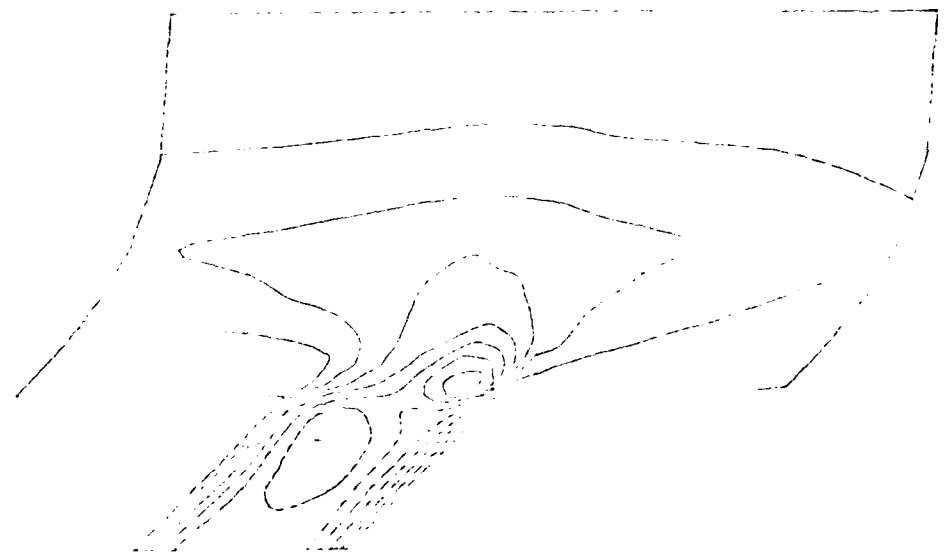


Fig. 2 - Vector Plot of Velocity in Vertical Symmetry Plane  
Bisecting Coolant Hole, 45° Injection.



(a) Streamwise Velocity Component



(b) Vertical Velocity Component

Fig. 3 - Contours of Velocity in Vertical Symmetry Plane  
Bisecting Coolant Hole, 45° Injection.

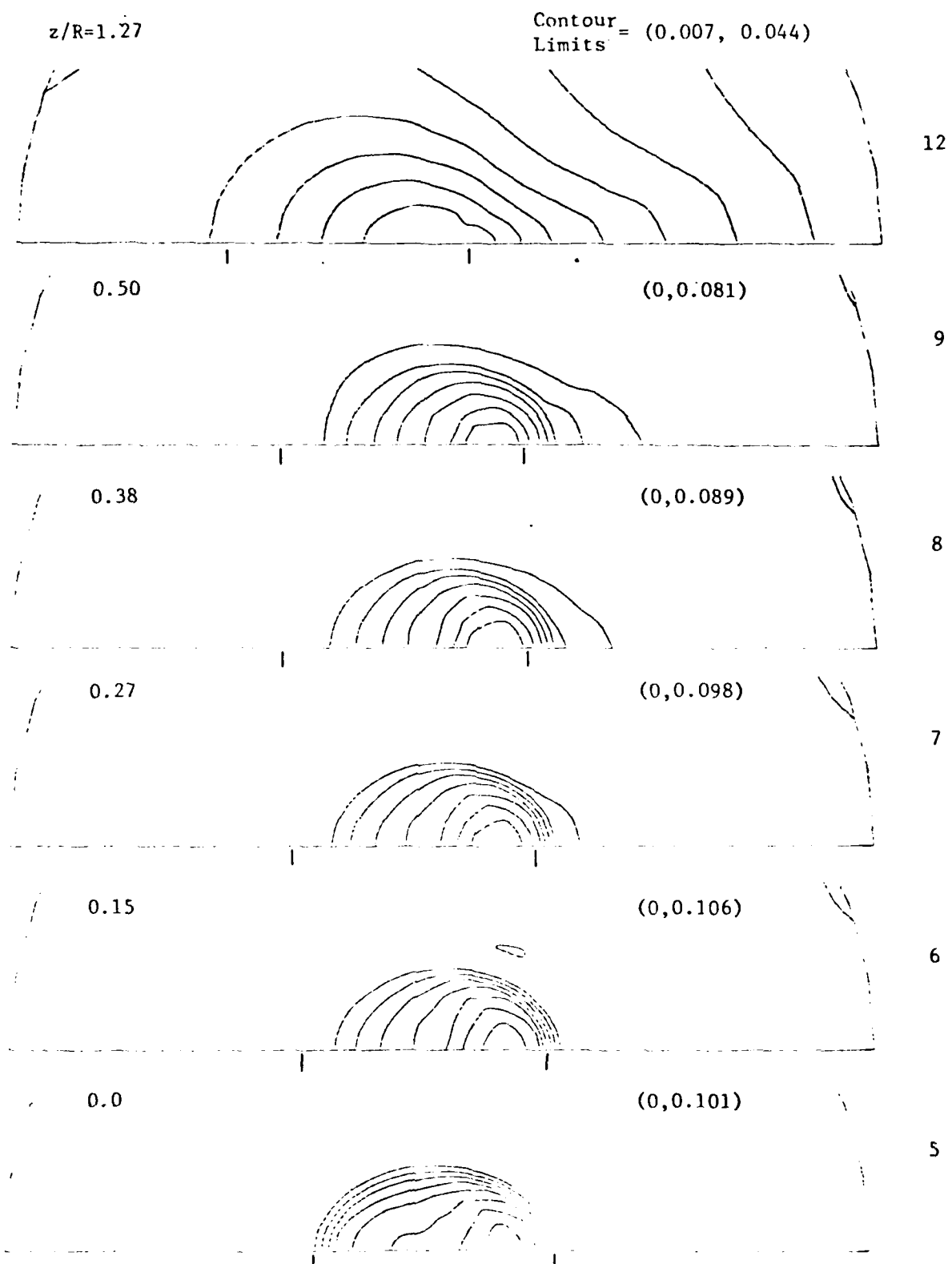


Fig. 4 - Contours of Vertical Velocity at Selected Planes Parallel to the Flat Surface, 45° Injection.

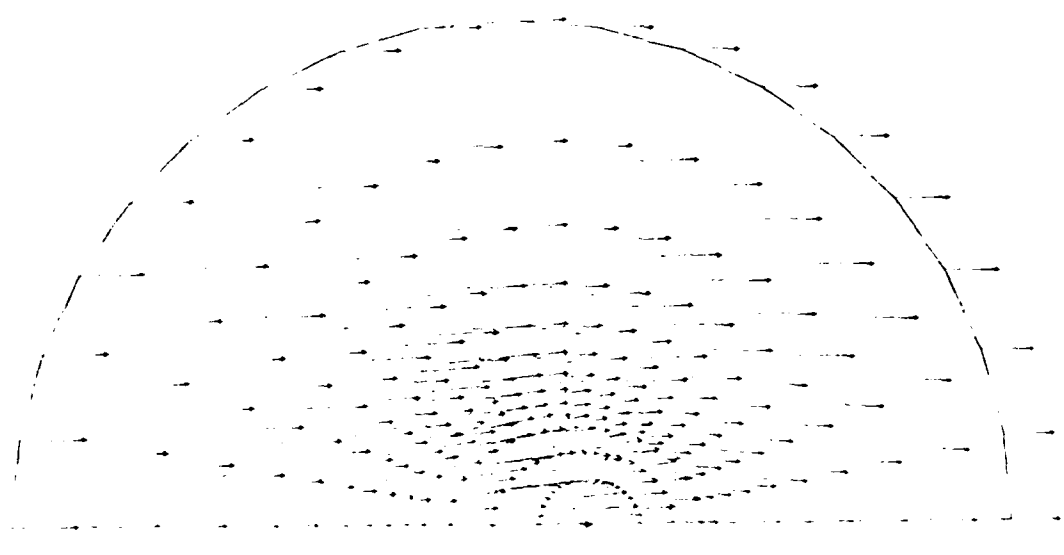
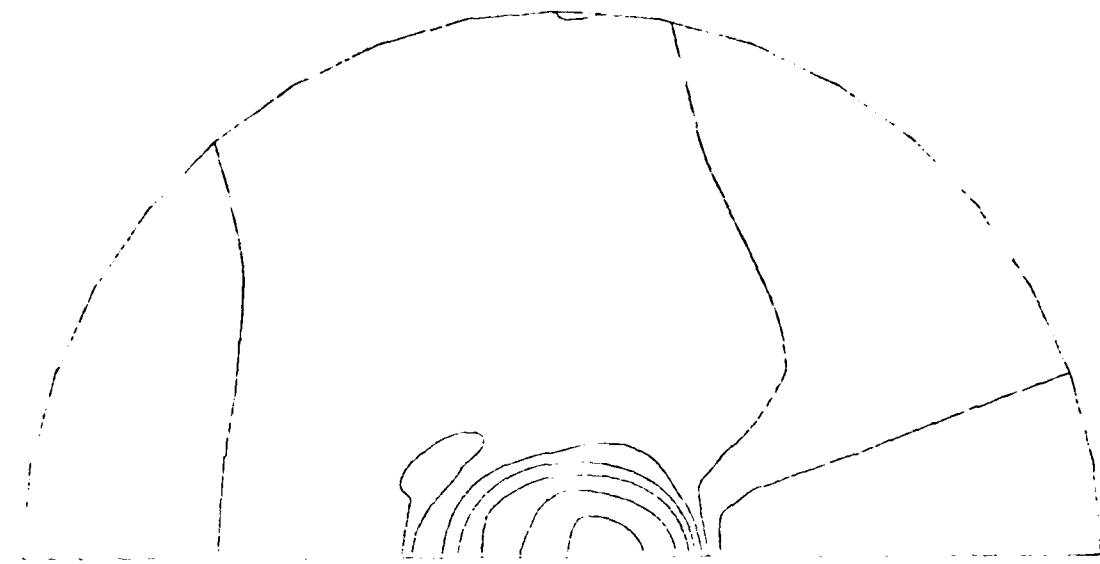


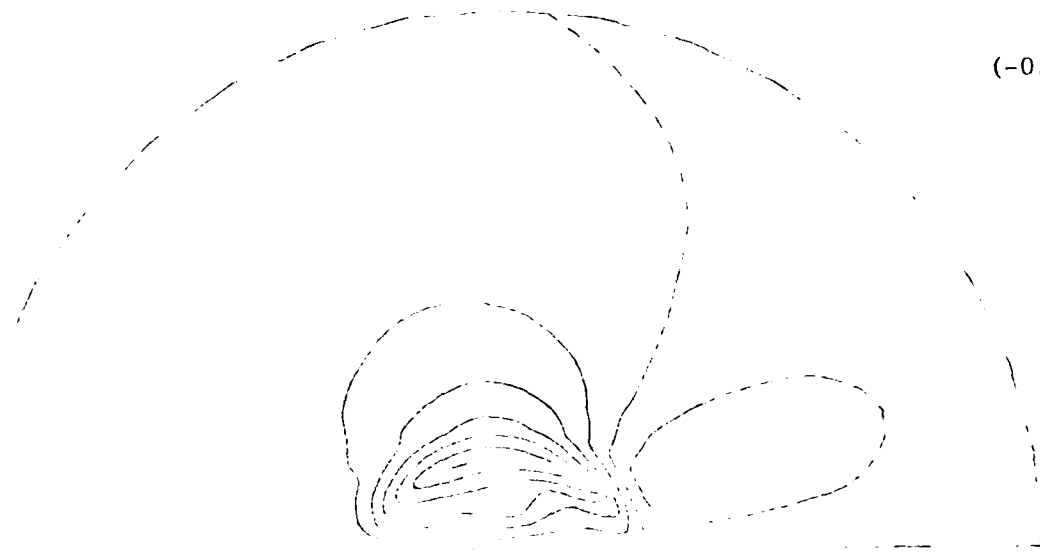
Fig. 5 - Vector Plot of Velocity in Horizontal Plane at  $z/R=0.15$ ,  
 $45^\circ$  Injection.

Contour Limits = (0.137, 0.258)



(a) Streamwise Velocity Component

(-0.012, 0.036)



(b) Transverse Velocity Component

Fig. 6 - Contours of Velocity in Horizontal Plane at  $z/R=0.15$ ,  
45° Injection.

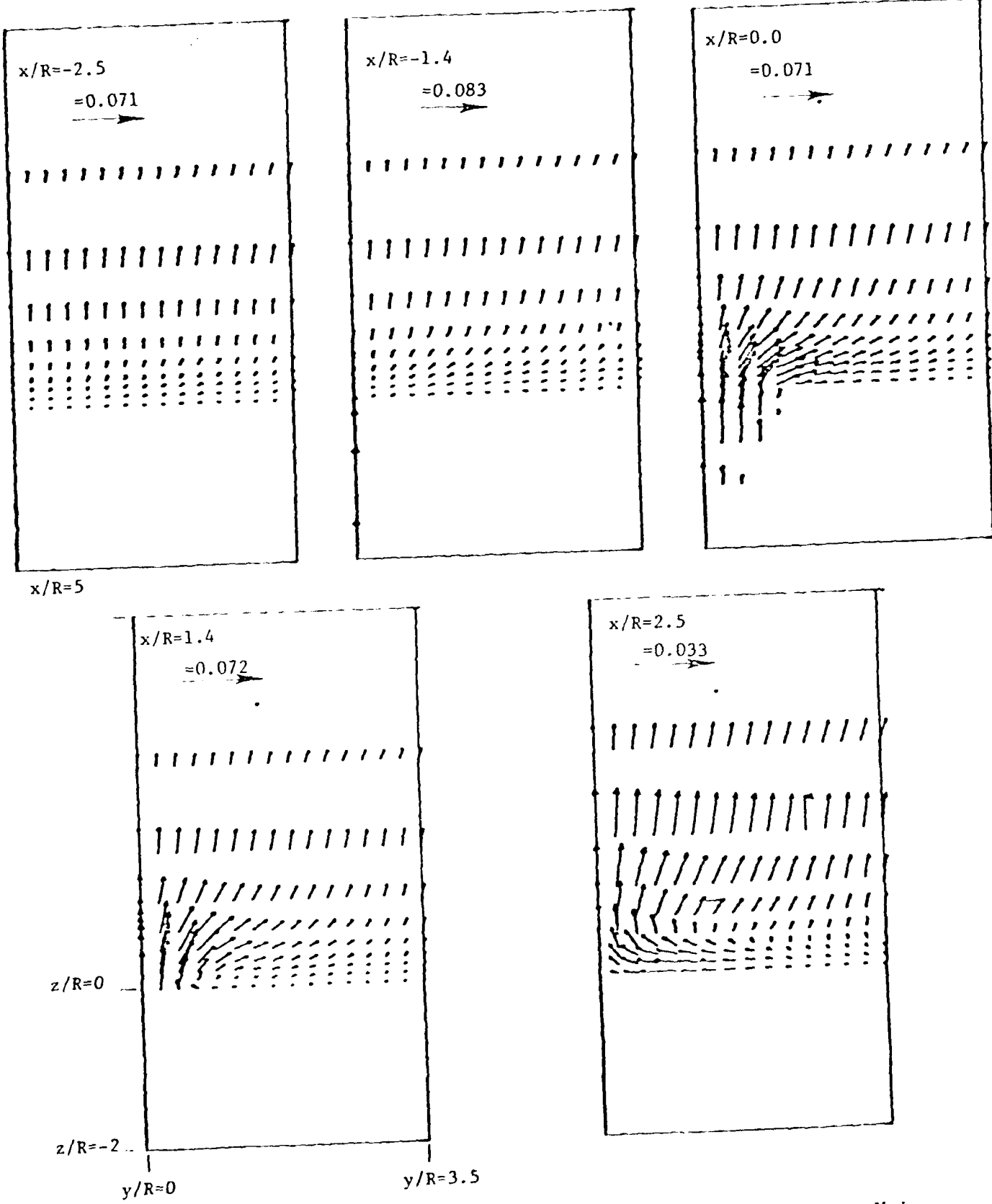


Fig. 7 - Secondary Velocity Vectors in Vertical Planes Perpendicular to Main Flow Direction, 45° Injection.

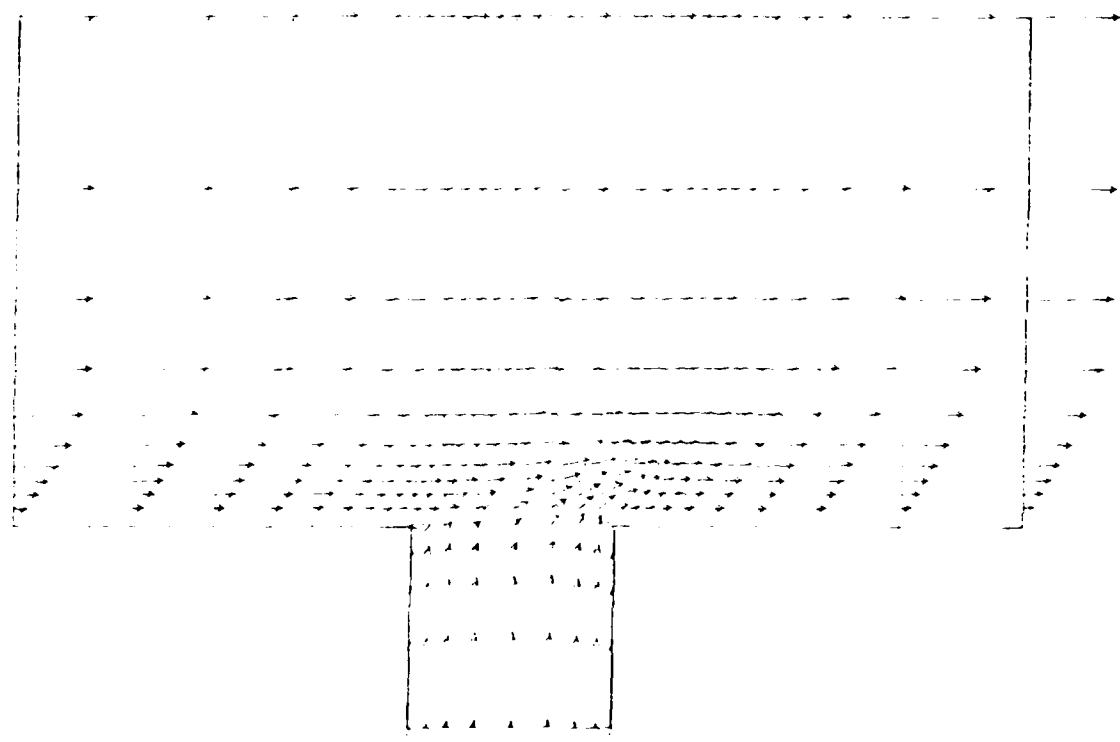


Fig. 8 - Vector Plot of Velocity in Vertical Symmetry Plane  
Bisection Coolant Hole, Normal Injection.

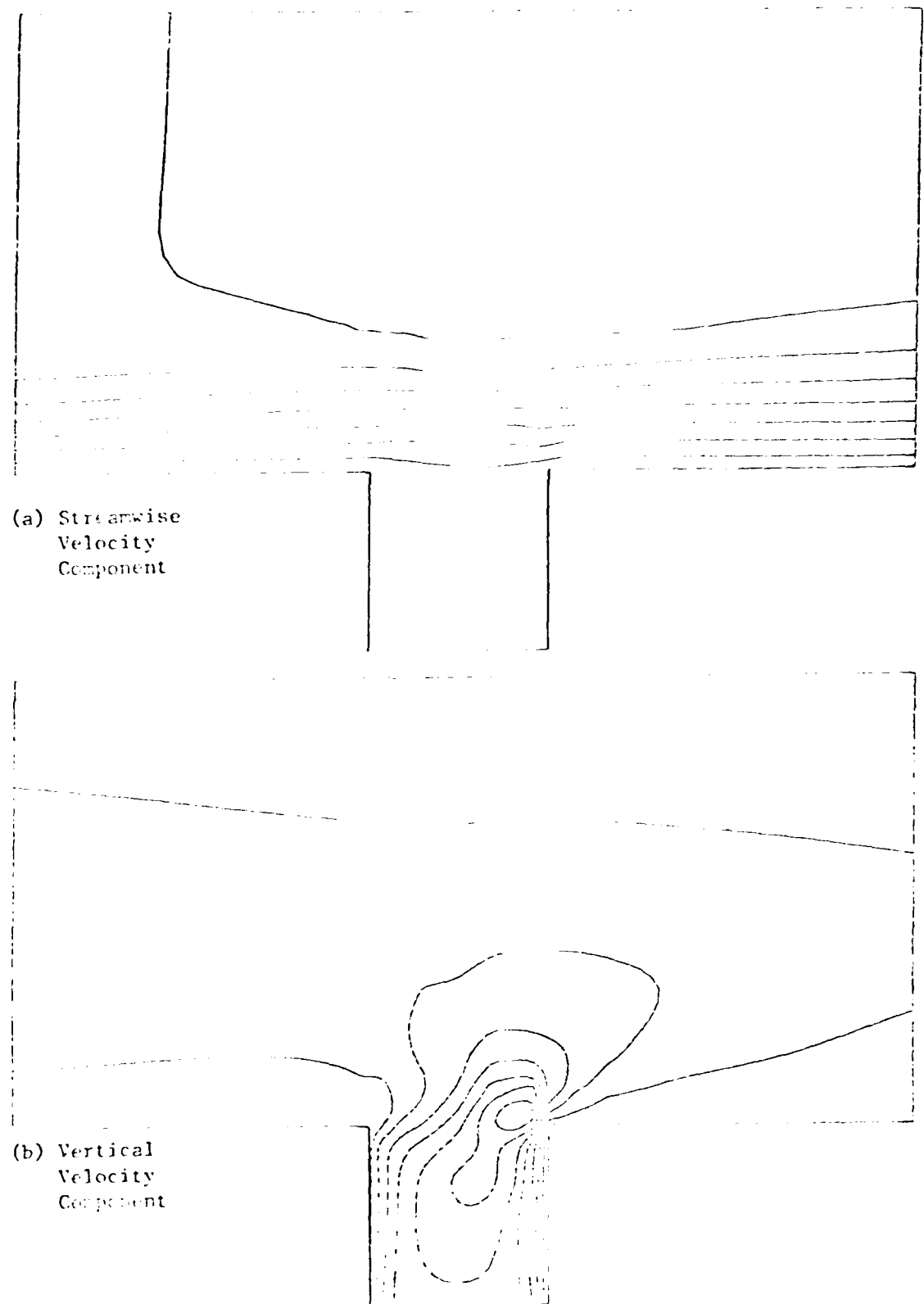


Fig. 9 - Contours of Velocity in Vertical Symmetry Plane Bisecting  
Coolant Hole, Normal Injection.

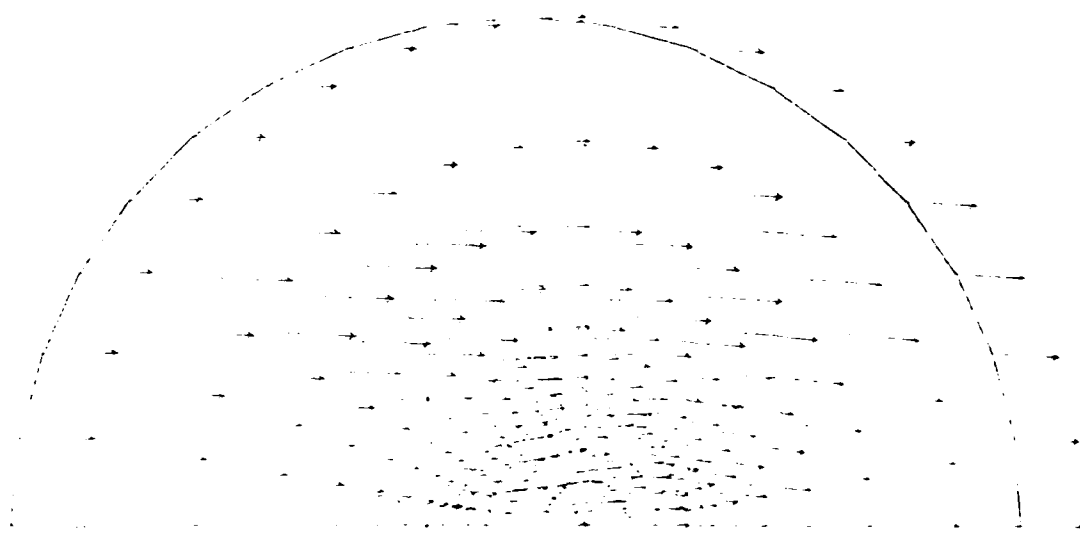


Fig. 10 - Vector Plot of Velocity in Horizontal Plane at  $z/R = 0.17$ ,  
Normal Injection.

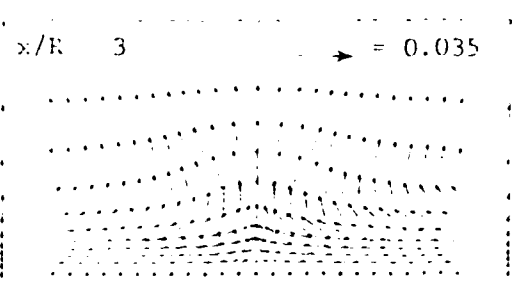
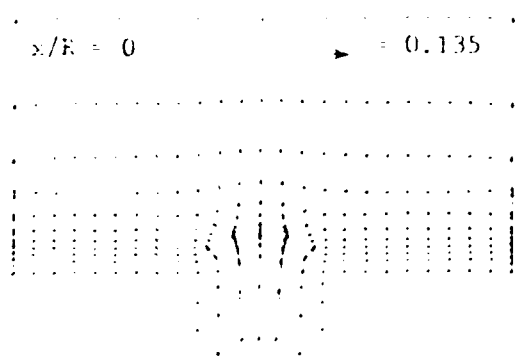
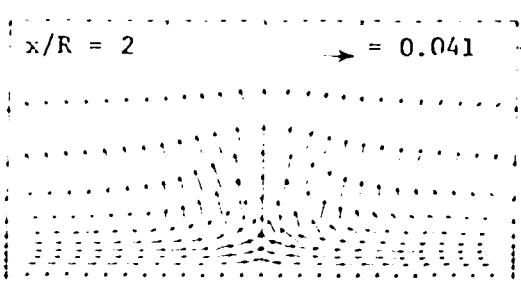
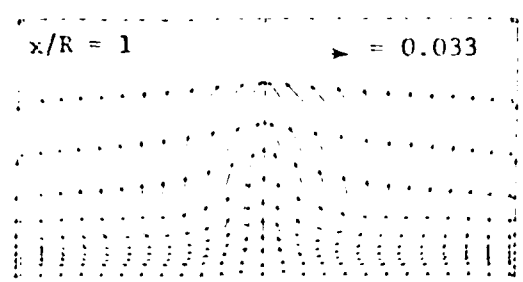
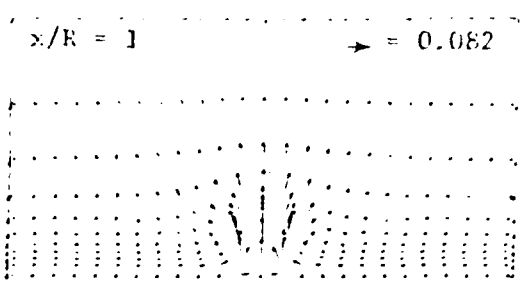
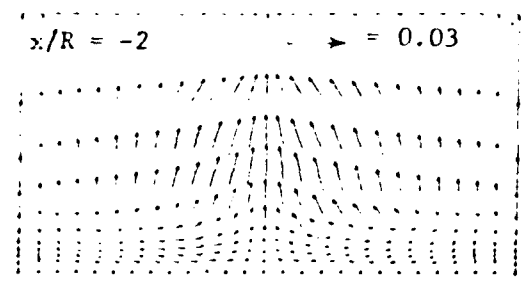


Fig. 11 - Secondary Velocity in Vertical Planes Perpendicular to Main Flow Direction, Normal Injection.

**DAL  
FILM**